Theoretical Study on the Gas-Phase Acidity of Multiple Sites of Cu^+−Adenine and Cu^{2+}−Adenine Complexes

Dianxiang Xing,*,†,‡ Xuejie Tan,‡ Xiaohua Chen,† and Yuxiang Bu*,†

Institute of Theoretical Chemistry, Shandong University, Jinan 250100, P. R. China, and School of Chemical Engineering, Shandong Institute of Light Industry, Jinan 250353, P. R. China

Received: January 11, 2008; Revised Manuscript Received: May 15, 2008

The acidities of multiple sites in Cu^+−adenine and Cu^{2+}−adenine complexes have been investigated theoretically. To compare, the acidities of adenine (A) and adenine radical cation ($A^{\bullet+}$) have also been included. The results clearly indicate that the acidities of C−H and N−H groups in $Cu^{+/2+}$−adenine are significantly enhanced relative to the neutral adenine. The acidic order for a given site on adenine and adenine derivatives is as follows: Cu^{2+}−adenine > $A^{\bullet+}$ > Cu^+−adenine > A. For Cu^+−adenine and Cu^{2+}−adenine, N3-coordination exhibits N9−H acid, and N1- and N7-coordination exhibits N6−H^a and N6−H^b acid, respectively. Additionally, it is found that C2−H group is surprisingly acidic in the coordination complexes. Calculations in aqueous solution reveal that our results can be extrapolated to aqueous solution. Analyses of the electronic properties interpret the highest acidity of Cu^{2+}−adenine among the adenine derivatives studied. Also, Electrostatic potential calculations of $[A(-H^+)]^-$ and $[A(-H^+)]^{\bullet}$ indicate that the removal of H^a or H^b from the amino group favors the bidentate coordination, which provides a dative bond from the deprotonated N and the original coordination ligand to copper ion besides the electrostatic interaction between them and thereby stabilizes the $[A(-H^+)]^-/[A(-H^+)]^{\bullet}$. NBO analysis confirms the electrostatic potential result.

Introduction

Metalcations are known to play an important role in both the stabilization and destabilization of DNA.[1–3] They could coordinate to the phosphate oxygen atoms as well as (very rarely) to sugar oxygen atoms and to electron donor groups of the bases and thereby influence the canonical DNA structures.[4] Metalation can not only change the probability for the formation of rare (minor) tautomers of bases[5–7] and modify the hydrogen bonding and the stacking that stabilizes the double helix[4a] but also could influence the ability of nucleobases to be deprotonated or protonated.[8–10] Consequently, such modifications of nucleobases could propagate into the formation of mispairs.[9,11–14] Among metal cations present in plants, animal and bacteria, copper is one of the most abundant transition metals.[15] In biochemistry, it takes part in the metabolism of iron and zinc and is involved in several redox reactions closely associated with DNA bases.[16–19] In aqueous solution, copper is susceptible to interact with nitrogen atoms of purine bases, and thus alters its acid−base properties of nucleobase atoms and group involved in complementary H-bond formation.[20,21]

Adenine, as an important nucleobase, acid−base properties of it and its derivatives are essential for understanding many mechanisms of basic importance in the biological process. It is well-known that the interaction energy between two bonded complementary nucleobases is dependent on the intrinsic basicity and acidity of the acceptor and donor groups.[22,23] In addition, gas-phase acidities of nucleobases combined with the knowledge of deprotonation sites, could also improve our understanding of chemical reactions basic to biological systems. Recently, exploration of copper(II) complexes as chemical nucleobases has seen an upsurge due to biologically accessible redox potential and high affinity toward nucleobases.

Considering the above situation it is surprising to find that there are only a few experimental studies that deal with the effects exerted by copper bound to a certain site of a nucleobase on other nearby sites.[4b,16,24] Although several theoretical studies have considered the interaction of guanine, adenine, uracil, and thiouracil with transition-metal cations (Ni^+, Cu^+, Cu^{2+})[9,16,24,25] and investigated the acidities of adenine and adenine derivatives,[22,23,26–29] to the best of our knowledge, no theoretical calculations have been carried out on the deprotonation of Cu^+−adenine and Cu^{2+}−adenine. In this paper, we mainly focus our attention on the influence of Cu^+ and Cu^{2+} coordination on the acidities of multiple sites in adenine. The geometrical characters, gas-phase acidities and electronic property of nondeprotonated and/or deprotonated complexes have been investigated. For the sake of comparison, the gas-phase acidity of adenine and adenine radical cation ($A^{\bullet+}$) have also been included.

Computational Method

The B3LYP/6-31+G** level of theory has been used throughout the optimizations, which has been shown to yield reliable geometries for a wide variety of system in particular for complexes containing transition metal cations.[30,31] All the possible geometries for the deprotonated $Cu^{+/2+}$−adenine conformers are fully optimized without any symmetry constraints on the basis of the optimized $Cu^{+/2+}$−adenine conformers available as displayed in Figure 1. Vibrational frequencies have been calculated at the same level to ensure the stationary point.

To further confirm the relative stabilities among the available conformers, single-point energy calculations have been performed at the B3LYP/6-311++G**// B3LYP/6-31+G** level

* To whom all correspondences should be addressed. E-mail: D.X.,xdx@mail.sdu.edu.cn; Y.B., byx@sdu.edu.cn.
† Shandong University.
‡ Shandong Institute of Light Industry.

10.1021/jp800256v CCC: $40.75
Published on Web 07/23/2008

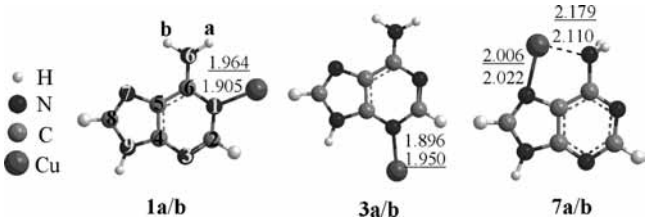

Figure 1. Optimized geometries of **1a/b**, **3a/b** and **7a/b**. **a** and **b** denote the Cu^+−adenine and Cu^{2+}−adenine complexes, respectively. Digits **1**, **3** and **7** denote the metal coordination sites N1, N3 and N7, respectively. Values with and without underlines are the Cu^{2+}−N and Cu^+−N distances, respectively.

of theory. The energies do not include the basis set superposition errors (BSSE), because BSSE corrections are usually small when the basis set expansion is sufficiently flexible,[32,33] which have no significant influence on the final energies.

For the following deprotonation process, $HB \rightarrow H^+ + B^-$, the enthalpy changes and Gibbs free energy changes can be calculated as

$$\Delta H = E(\mathrm{HB}) - E(\mathrm{B}^-) - E(\mathrm{H}^+) + \Delta(\mathrm{PV}) = E(\mathrm{HB}) - E(\mathrm{B}^-) + E_{\mathrm{vib}}(\mathrm{HB}) - E'_{\mathrm{vib}}(\mathrm{B}^-) - (5/2)RT \quad (1)$$

$$\Delta G = \Delta H - T\Delta S \qquad (\Delta S = S(\mathrm{HB}) - S(\mathrm{B}^-) - S(\mathrm{H}^+)) \quad (2)$$

where $E(i)$, $E'_{\mathrm{vib}}(i)$ and $S(i)$ refer to the total energy, zero-point vibrational energy (ZPVE) also including the thermal vibrational corrections to the total energy for simplicity, and entropy of the species i, respectively. The $(5/2)RT$ term includes the translation energy of the proton and the Δ(PV) term. As a rule, GPA is defined as the negative value of the Gibbs energy changes, that is, GPA $= -\Delta G$. Obviously, the larger the value of GPA is, the weaker the HB acidity is.

Interaction energies between the adenine and $Cu^{+/2+}$ ion are calculated as the difference between the energy for the complex and those for the individual molecules that constitute it,

$$\mathrm{MIA} = H(\mathrm{A}) + H(\mathrm{M}^{n+}) - H(\mathrm{M}^{n+}\text{−A}) + H'(\mathrm{A}) + H'(\mathrm{M}^{n+}) - H'(\mathrm{M}^{n+}\text{−A})$$

where H(A), $H(\mathrm{M}^{n+})$ and $H(\mathrm{M}^{n+}$−A) refer to the energy of adenine, $Cu^{+/2+}$ ion and the total $Cu^{+/2+}$−adenine complex, and H'(i) refers to the corresponding zero-point vibrational energy (ZPVE) and zero point energy.

Also, natural bond orbital (NBO) approach implemented in Gaussian 03 has been used to evaluate the interactions between orbitals of the base and orbitals of the metal involved in the dative bonds from the former to the latter and possible back-donations from the latter to the former.[34–37] The calculations were performed at the B3LYP/6-311++G**// B3LYP/6-31+G** level.

To explore the solvent effects of aqueous solution on the calculated GPAs in the deprotonation processes, some structures including metal complexes and their deprotonated structures have been optimized by employing polarized continuum model (PCM)[38] at the B3LYP/6-31+G** level of theory and the final energies in aqueous solution are computed at the B3LYP/6-31+G** level, because the preliminary calculations of the energy difference between the B3LYP/6-31+G** and B3LYP/6-311++G** levels in the gas phase show that the energy gap is less than 1.3 kcal/mol.

TABLE 1: Metal Ion Affinities (MIA) of Cu^+−Adenine and Cu^{2+}−Adenine Complexes[a]

	1a	3a	7a	1b	3b	7b
ΔE, kcal/mol	1.30	1.36	0	1.55	0	18.41
MIA	65.03	65.10	66.71	266.41	268.02	249.71

[a] ΔE is the relative energy including zero point and ZPVE, which are calculated at the B3LYP/6-311++G**// B3LYP/6-31+G**.

TABLE 2: Relative Energies (kcal/mol) of the Different Deprotonated Conformers of Cu^+−Adenine and Cu^{2+}−Adenine[a]

	ΔE		ΔE		ΔE
1aC2	18.80	**3aC2**	18.80	**7aC2**	78.32
1aN6a	5.03	**3aN6a**	37.94	**7aN6a**	
1aN6b	27.62	**3aN6b**	37.77	**7aN6b**	0
1aC8	65.10	**3aC8**	62.75	**7aC8**	39.28
1aN9	22.04	**3aN9**	4.27	**7aN9**	8.23
1bC2	22.47	**3bC2**	22.13	**7bC2**	23.78
1bN6a	3.60	**3bN6a**	29.10	**7bN6a**	
1bN6b	20.59	**3bN6b**	27.94	**7bN6b**	0
1bC8	32.96	**3bC8**	32.41	**7bC8**	32.39
1bN9	26.73	**3bN9**	10.18	**7bN9**	34.74

[a] The relative energies of Cu^+−adenine(−H^+) and Cu^{2+}−adenine(−H^+) are calculated relative to **7aN6b** and **7bN6b**, respectively.

TABLE 3: Gas-Phase Acidities of Adenine and Adenine Radical Cation, Corresponding to Deprotonation from C2, N6, C8 and N9 Sites (GPA in kcal/mol)

	Adenine (A)				
	$[A(C2)]^-$	$[A(N6a)]^-$	$[A(N6b)]^-$	$[A(C8)]^-$	$[A(N9)]^-$
GPA	390.56	348.40	347.83	366.36	330.52
	Radical Cation ($A^{\bullet+}$)				
	$[A(C2)]^\bullet$	$[A(N6a)]^\bullet$	$[A(N6b)]^\bullet$	$[A(C8)]^\bullet$	$[A(N9)]^\bullet$
GPA	226.23	221.03	219.84	233.14	216.84

TABLE 4: Gas-Phase Acidities (kcal/mol) of Cu^+−Adenine and Cu^{2+}−Adenine Complexes, Corresponding to Deprotonation from C2, N6, C8 and N9 Sites[a]

	GPA		GPA		GPA
1aC2	241.64	**3aC2**	241.28 (291.56)	**7aC2**	299.35
1aN6a	229.54(280.91)	**3aN6a**	260.22 (292.73)	**7aN6a**	
1aN6b	250.00	**3aN6b**	259.89 (292.57)	**7aN6b**	225.63 (245.53)
1aC8	286.38	**3aC8**	282.82 (311.65)	**7aC8**	263.68
1aN9	246.17	**3aN9**	227.15 (275.62)	**7aN9**	233.63
1bC2	133.67 (263.91)	**3bC2**	136.40	**7bC2**	120.62
1bN6a	116.03 (251.08)	**3bN6a**	141.10	**7bN6a**	
1bN6b	131.80 (259.14)	**3bN6b**	140.00	**7bN6b**	95.80 (200.82)
1bC8	144.90 (275.61)	**3bC8**	146.72	**7bC8**	129.00
1bN9	136.97 (261.78)	**3bN9**	123.69 (262.43)	**7bN9**	127.37

[a] Values in parentheses are GPAs in aqueous solution calculated using PCM model.

All the computations have been performed at 298.15 K and 1.0 atm using the Gaussian 03 program, and the SCF convergence criteria *Tight* has been used throughout the calculations.[39,40]

Results and Discussion

The calculated metal ion affinities for the $Cu^{+/2+}$−adenine complexes are listed in Table 1. The relative energies and the corresponding gas-phase acidities of all species studied in the deprotonation process are summarized in Tables 2, 3 and 4, respectively. Table 5 lists the partial charges on each fragment of the coordination complexes. The optimized $Cu^{+/2+}$−adenine complexes and deprotonated $Cu^{+/2+}$−

TABLE 5: NBO Partial Charge on Each Fragment of the Cu^+−Adenine and Cu^{2+}−Adenine Complexes

	1a	3a	7a	1b	3b	7b
adenine	0.17	0.16	0.13	1.09	1.07	0.90
$Cu^{+/2+}$	0.82	0.84	0.87	0.91	0.93	1.10

adenine ($Cu^{+/2+}$−adenine(−H^+)) conformers are presented in Figures 1 and 2, respectively. Figure 3 depicts the dependencies of GPAs on the deprotonation sites of all species studied. The spin densities and molecular orbitals of adenine radical cation ($A^{\bullet+}$) and Cu^{2+}−adenine complexes are displayed in Figures 4 and 5, respectively. Figure 6 displays the electrostatic potential of deprotonated adenine ($[A(-H^+)]^-$) and deprotonated adenine radical cation ($[A(-H^+)]^\bullet$) species.

For simplification, the following notations are adopted in the paper: **a** and **b** stand for the Cu^+−adenine and Cu^{2+}−adenine complex, respectively. The coordination sites N1, N3 and N7 atoms on adenine are simplified as **1**, **3** and **7**, respectively. For example, **1a** indicates that Cu^+ interacts with adenine through N1 atom. To this initial notation, **C2**, **N6a**, **N6b**, **C8** and **N9** are added to denote the loss of a proton from the corresponding site of adenine, respectively. Here, **N6a** or **N6b** means the loss of the proton H^a or H^b attached to amino N atom. Also, the same suffix in parentheses is added at the back of A or $A^\bullet$ to denote its deprotonation. For example, $[A(C2)]^\bullet$ stands for the removal of a proton from C2 site of adenine radical cation ($A^{\bullet+}$).

To better evolve the deprotonation process of $Cu^{+/2+}$−adenine, the relevant geometries and the relative stabilities of the coordination compounds are depicted first. As is shown in Figure 1, each Cu^+−adenine and Cu^{2+}−adenine gives three conformers, i.e., **1a**, **3a**, **7a** and **1b**, **3b**, and **7b**. Among them, **1a/b** and **3a/b** are planar geometries, in which Cu^+/Cu^{2+} interacts with adenine N1 and N3 atoms, respectively (r_{Cu-N1} = 1.905 Å for **1a**, and 1.964 Å for **1b**; r_{Cu-N3} = 1.896 Å for **3a**, and 1.950 Å for **3b**). The dihedral angles Cu−N1−C2−N3 and Cu−N3−C2−N1 are near zero, and the total angles of the three bonds around the N6 atom are 360°. **7a/b** is bidentate with N7 and N6 of the amino group (r_{Cu-N6} = 2.110 Å, r_{Cu-N7} = 2.022 Å for **7a** and r_{Cu-N6} = 2.179 Å, r_{Cu-N7} = 2.006 Å for **7b**). Moreover, N7-coordination changes the amino group from a planar to a pyramidal form. The total bond angles of the three bonds around the N6 are 324.2° for **7a** and 326.6° for **7b**. On the other hand, comparison of the $Cu^{+/2+}$−N bond lengths reveals that Cu^{2+}−N is generally longer than the corresponding Cu^+−N (Figure 1).

Among the three Cu^+−adenine complexes, **7a** is the most stable structure; **1a** and **3a** are about 1.30 and 1.36 kcal/mol higher in energy than **7a**, respectively (Table 1). For Cu^{2+}−adenine complexes, **7b** is the least stable conformer. It is ∼18.41 kcal/mol higher in energy than **3b**, the most stable Cu^{2+}−adenine conformer. **1b** is ∼1.55 kcal/mol less stable than **3b**. Actually, the same result has also been found by Russo et al.[25a] The predicted metal ion affinities also reflect the relative stabilities of these complexes. Here, it is worth mentioning that MIAs of **7a** (66.7 kcal/mol, Table 1), **3a** (65.1 kcal/mol) and **3b** (268.0 kcal/mol) compare well with the results (69.0 kcal/mol for **7a,** 67.2 kcal/mol for **3a**[16,25b] and 269.1 kcal/mol for **3b**[25a]) obtained by Russo and Sodupe et al. employing B3LYP/6-311+G(2df,2p) or 6-311++G(3df,2pd) basis set. This clearly indicates that our basis sets are reliable and efficient in this study. Thus, B3LYP/6-311++G**//B3LYP/6-31+G** level of theory is employed in the following discussion.

On the other hand, bonding analysis of **7a** shows that the $3d_{xz}$ orbital has much overlap with the adenine N7 and N6 than the other four orbitals; for 3a, $3d_{z^2}$ orbital has much overlap with the adenine N3, the lowest electronic states of both structures are $^1A'$. These findings are in agreement with the analysis carried out by Sodupe et al.[25b] As for Cu^{2+}−adenine, the preferred coordination is adenine N3 (i.e., planar 3b). The lowest electronic state is $^2A'$ derived from A^+. The $3d_{z^2}$ (a′) orbital has much overlap with the adenine N3, because the lobule of $3d_{z^2}$ positions toward the adenine N3.

Geometries and Relative Stabilities. All the possible geometries of the deprotonated $Cu^{+/2+}$−adenine are obtained on the basis of the six optimized conformers mentioned above. Five geometries are initially designed for each conformer, which correspond to the loss of one of the protons attached to adenine C2, N6 (two protons H^a and H^b bound), C8 and N9 atoms. Optimizations reveal that, except for **7a/b**, there are five deprotonated structures for each **1a/b** and 3**a/b** as displayed in Figure 2. For **7a** and **7b**, each gives four geometries, because the removal of H^a and H^b from N6 is converged to the same conformer during the geometry optimization. Considering the lack of structural information experimentally, it is necessary to describe the geometrical changes for $Cu^{+/2+}$−adenine upon deprotonation before discussing the gas-phase acidities (GPAs) of the coordination complexes. As mentioned above, there are five active deprotonation sites on adenine in $Cu^{+/2+}$−adenine conformers. Deprotonation occurring at different position can result in significantly different geometrical changes for $Cu^{+/2+}$−adenine complexes.

As shown in Figure 2, in **1a/bC2**, Cu^+/Cu^{2+} is monodentate with C2 rather than with the original N1 because Cu^+/Cu^{2+} sits much closer to C2 than to N1. Compared with **1a** and **1b**, the Cu−ligand distances are shortened by 0.006 and 0.058 Å, respectively. In addition, **1aC2** still remains the original planarity, but **1bC2** loses it. The Cu−C2−N3−C4 dihedral angle of **1bC2** is 161.1°. Similarly, **1a/bN6a**, obtained by the loss of the proton H^a from N6, corresponds to a bidentate form in which Cu^+/Cu^{2+} interacts with N1 and N6. The Cu−N1 distances are significantly weakened, where the increments in bond length are about 0.223 Å for **1aN6a** and 0.307 Å for **1bN6a**. Both deprotonated structures are essentially planar. On the other hand, the structure **1a/bN6b**, formed by removing another proton (H^b) from N6, corresponds to a monodentate form in which metal ion bonds with N1. The Cu−N1 bonds are greatly strengthened relative to **1a/b**, respectively. Also, both **1aN6b** and **1bN6b** are planar. For **1a/bC8** and **1bN9**, copper ion is monodentate with N1. The decreases in bond length (∼0.004/0.056 Å and 0.051 Å, respectively) clearly illustrate the enhanced strength of Cu−N1 bond. In **1aC8**, the Cu−N1−C2-N3 dihedral angle is 165.8°. The total angle of the amino group is 339.1°. **1bC8** and **1bN9** are planar geometries. For **1aN9**, it is surprising to find that Cu^+ slightly moves toward the amino group and behaves as a bidentate form with N1 and N6 (Figure 2). Accordingly, the amino group is converted into a pyramid (the total angle of the amino is 326.3°).

For the deprotonation of **3a/b**, optimization reveals that each can also generate five conformers as displayed in Figure 2, in which three correspond to C2-, C8- and N9-deprotonation, and two correspond to N6-deprotonation. In **3aC2**, Cu^+ appears to be monodentate with C2 instead of the original N3. Structurally, **3aC2** is exactly the same as **1aC2**, indicating that C2, which is negatively charged after deprotonation, is more favorable for Cu^+ attaching than neutral N1 or N3. Similarly, in **3aN9**, Cu^+ is monodentate with N9, a negatively charged atom, instead of original N3. Except for **1aC2** and **3aN9**, other deprotonated

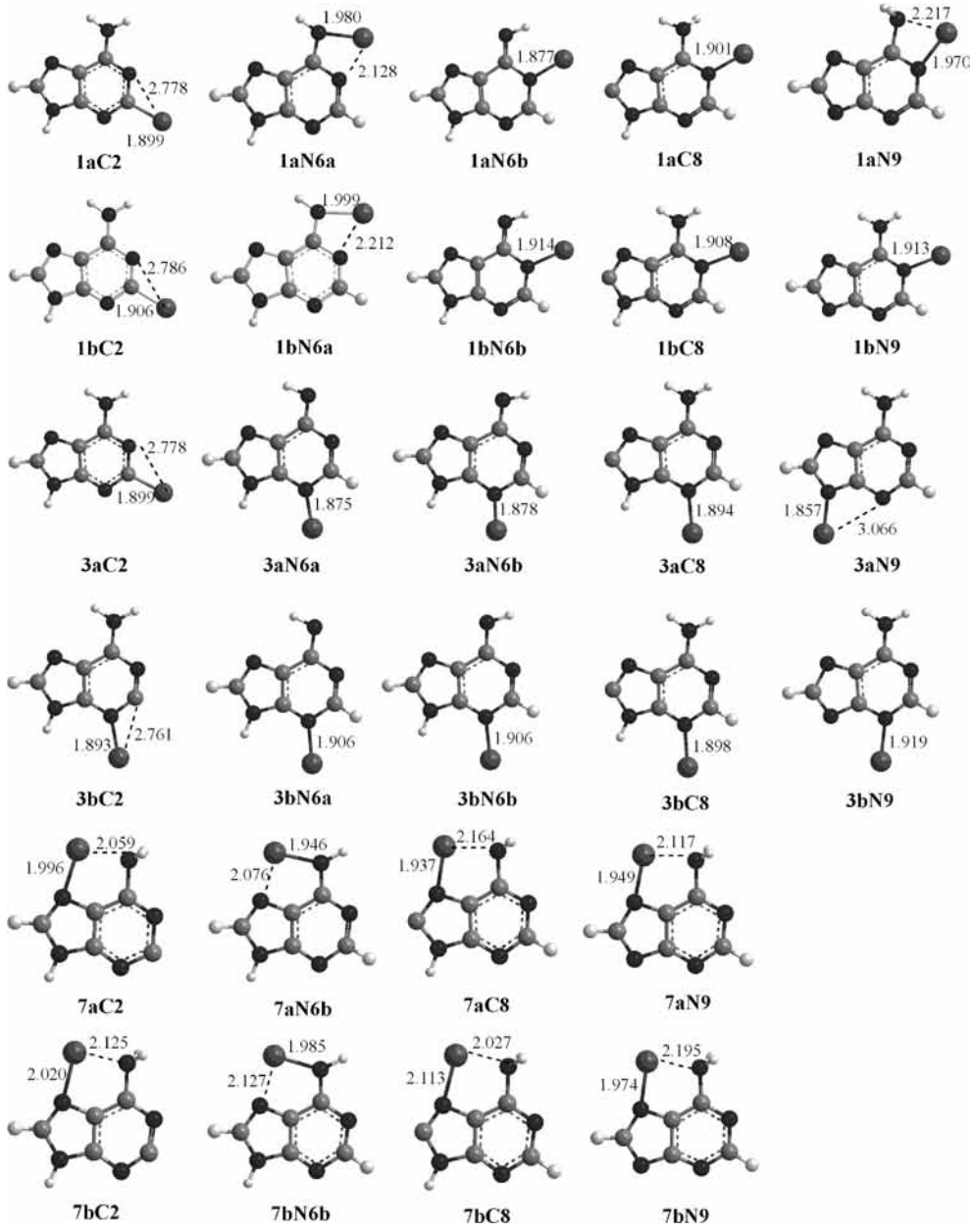

Figure 2. Optimized geometries of Cu^+−adenine(−H^+) and Cu^{2+}−adenine(−H^+), calculated at the B3LYP/6-31+G** level.

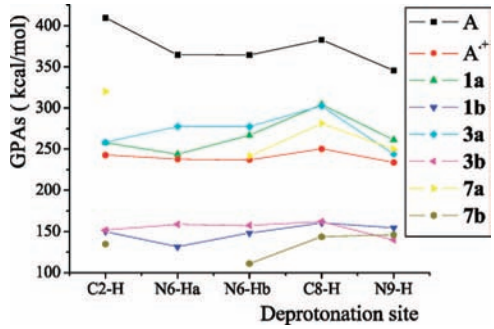

Figure 3. Dependencies of GPAs on deprotonation sites of the adenine and adenine derivatives.

conformers correspond to a monodentate form in which copper ion interacts with the original N3. All the Cu−N3 (or Cu−N9 for **3aN9**) bonds in the deprotonated conformers are significantly strengthened relative to that in **3a/b**. This is in line with our usual understanding when considering that deprotonated adenine and metal ion are charged oppositely. Moreover, Cu^{2+}−ligand distance is generally longer than Cu^+−ligand in these deprotonated structures. In addition, Cu^+ or Cu^{2+} still remains in the same plane with adenine fragment except for **3aN6a** and **3aN6b** conformers. The dihedral angles of Cu−N3−C2−N1 are −152.2 ° for **3aN6a** and −150.6 ° for **3aN6b**.

For **7a** and **7b**, each gives four deprotonated structures rather than five (Figure 2), which are named as **7aN6b** and **7bN6b**. Geometrically, all deprotonated conformers are characterized by a bidentate form (with N7 and N6). Compared with Cu−N6 and Cu−N7 bonds in **7a/b**, these bond distances are shortened with the exception of Cu−N6 bond in **7aC8** and **7aN9**. Additionally, in **7a/bC2**, **7a/bC8** and **7a/bN9**, copper remains in the same plane with adenine ring atoms, but the amino group behaves as a pyramidal type. In **7a/bN6b**, all atoms are essentially in the same plane.

The relative energies in Table 2 clearly indicate that for a certain deprotonation site, the conformer that corresponds to deprotonation from the atom adjacent to Cu^+ or Cu^{2+} is usually more stable than those remote to the metal ion. That is, **1a/**

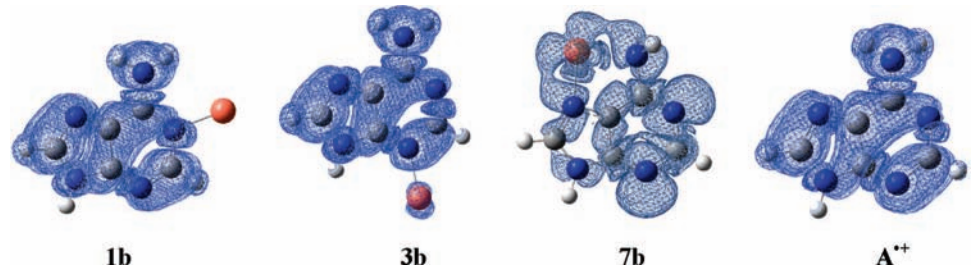

Figure 4. Spin densities of Cu^{2+}−adenine complexes and the adenine radical cation ($A^{\bullet+}$), calculated at the B3LYP/6-311++G** with isovalue of 0.0004.

Figure 5. Molecular orbitals of Cu^{2+}−adenine complexes and $A^{\bullet+}$, calculated at the B3LYP/6-311++G** with isovalue of 0.002.

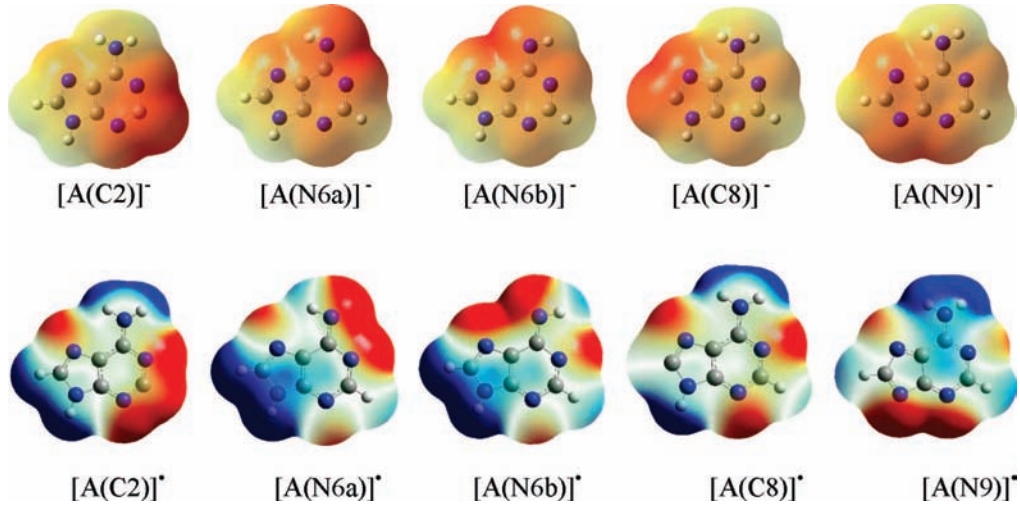

Figure 6. Electrostatic potential of deprotonated A ($[A(-H^+)]^-$) and deprotonated $A^{\bullet+}$ ($[A(-H^+)]^\bullet$), calculated at the B3LYP/6-311++G** with isovalue of 0.0004.

bC2 and **3a/bC2** are more stable than **7a/bC2**, whereas **7a/bC8** is more stable than **3a/bC8** and **1a/bC8**. Similar situations are observed for N6- and N9-deprotonation, in which **7a/bN6b**, **1a/bN6a** and **3a/bN9** are more stable. This is consistent with our usual understanding. In the following section, further explanation is provided by electrostatic potential. Among all Cu^+−adenine(−H^+) structures, the first three most stable ones are as follows: **7aN6b** > **3aN9** ≥ **1aN6a**. **3aN9** and **1aN6a** are 4.27 and 5.03 kcal/mol higher in energy than **7aN6b**, respectively. This order is identical to the relative stabilities of the Cu^+−adenine complexes. For deprotonated Cu^{2+}−adenine species, the first three most stable conformers are: **7bN6b** > **1bN6a** > **3bN9**, where **7bN6b** is 3.60 and 10.18 kcal/mol lower in energy than **1bN6a** and **3bN9**, respectively (Table 2). This is at variance with the relative stabilities of Cu^{2+}−adenine complexes, where the relative stabilities of Cu^{2+}−adenine complexes follow the order: **3b** > **1b** > **7b**. The relative stabilities of the deprotonated structures could be further interpreted by employing natural bond orbital (NBO).

GPAs. The gas-phase acidities for the neutral adenine, adenine radical cation and $Cu^{+/2+}$−adenine are summarized in Tables 3 and 4, respectively. The dependencies of the GPAs on deprotonation sites of all species studied are displayed in Figure 3.

It can be seen from Table 3, the N9−H group is the most acidic site of adenine with GPA of 330.52kcal/mol, followed by N6−H^b and N6−H^a groups. The GPA of N6−H^b and N6−H^a groups are 347.83 and 348.40 kcal/mol, respectively. The C8−H and C2−H are the two least acidic groups. Actually, the acidic order of these five groups is very consistent with the result obtained by employing the B3LYP/6-31+G** or B3LYP/6-31+G* level of theory.[22,29] There are some significant changes, however, as far as the acidity of adenine radical cation is concerned. As is expected, adenine radical cation is much more acidic than the neutral adenine (Figure 3), which can be seen from the significant decreases of GPAs (Table 3). But still in all active sites, N9−H, N6−H^b and N6−H^a groups are the first three acidic groups as in the neutral adenine, whereas the last two groups is opposite to that in neutral adenine.

Also, examination of the GPA values of $Cu^{+/2+}$−adenine complexes reveals the expected behavior for the acidity, i.e., all of the C−H and N−H groups, especially the C−H and N−H groups on Cu^{2+}−adenine are greatly acidified relative to the neutral adenine (Table 4, GPA). The GPAs of the active groups

on Cu^{2+}−adenine are significantly decreased to 95.80−146.72 kcal/mol. Consistent with the observation on the relative stabilities, for a certain acidic group, the regions close to metal cation are usually more acidic than the regions remote to it. As compared with the active groups on adenine and adenine radical cation, however, only for **3a/b**, N9−H group still remains the most acidic site (GPA is 227.15 /123.69 kcal/mol), whereas the most acidic site for **1a/b** is N6−H^a group (with GPA of 229.54 /116.03 kcal/mol) and for **7a/b** is N6−H^b group (with GPA of 225.63 /95.80 kcal/mol). As mentioned above, these four stable deprotonated structures (**1a/bN6a** and **7a/bN6b**) are all bidentate with N1 and N6 or with N7 and N6. Additionally, it is unexpected to find that the metal coordination greatly increases the acidity of C2−H group and make it be the second acidic site in **1a**, **3a/b** and **7b**. Even in **1b**, C2−H is the third acidic group, which is only ∼1.9 kcal/mol less acidic than the second acidic group, N6−H^b. On the contrary, for the free adenine, C2−H with GPA of 390.56 kcal/mol is the least acidic group and its acidity is slightly higher than that of benzene proton, 401.7 kcal/mol.[29b] In **1a/b**, **3a/b** and **7a/b**, however, the acidities of the C2−H group are 241.64/133.67, 241.28/136.40 and 299.35/120.62 kcal/mol, respectively, which are much higher than the aromatic proton. Similar noticeably enhanced acidity of the C2−H group has also been found in 3-methyladenine (GPA of C2−H in 3-methyladenine is 368.8 kcal/mol[29b]). This is not surprising given the fact that the adenine derivatives are positively charged. Comparison of the GPAs of A, $A^{\bullet+}$ and coordination complexes reveals that the relative acidities are as follows: Cu^{2+}−adenine > $A^{\bullet+}$ > Cu^+−adenine > A (Figure 3), in which the acidity of Cu^{2+}−adenine is much higher than that of Cu^+−adenine, indicating that divalent copper cation has greater effect on adenine acidity than monovalent cation. Moreover, coordination of Cu^{2+} greatly decreases the GPA gap between the most acidic group and the least one with respect to that in the neutral adenine (60.04 kcal/mol). The GPA gap ranges from 23.0 to 33.2 kcal/mol, depending on the coordination sites. For Cu^+ coordination, the GPA gaps between the most acidic group and the least one are 56.84 (**1a**), 55.67 (**3a**) and 73.72 kcal/mol (**7a**), respectively. Such dependencies of the acidities on the metal coordination region and oxidation state of copper suggest that the acidities of the active groups could be controlled by modulating the metal coordination site or the metal cation.

Additionally, to explore the solvent effect of an aqueous solution on the deprotonation processes and thus to verify that our results can be extrapolated to aqueous solution, we have chosen one of the $Cu^{2+/+}$−adenine (**1b** and **3a** systems) at random and computed their GPAs of various active sites on **1b** and **3a** systems. In addition, the GPA of the most acidic group of the complex for each coordination site has been calculated. The same level of the calculation shows that in aqueous solution, the complexes and the deprotonated forms become more stable by solvation. However, the undeprotonated form is much better stabilized than its deprotonated forms for each coordination site. As listed in Table 4, comparisons of the GPAs of **1b** and **3a** in aqueous solution clearly indicate that the N6−Ha and N9−H groups are still the most acidic groups of all active sites on **1b** and **3a**, respectively. Moreover, the acidic order of various active sites still follows the same order as that in the gas phase. Therefore, it can be deduced that the other system of the metal complex should have the same result. Also, it reveals that our results could be extrapolated to aqueous solution. The GPAs of the most acidic group for the other systems in aqueous solution are also displayed in Table 4. However, comparison of GPAs of Cu^{2+}−adenine and Cu^+−adenine complexes shows that the gap of GPAs is decreased in aqueous solution, in spite of this, the Cu^{2+}−adenine complex is more acidic than Cu^+−adenine complex.

Electronic Properties. To highlight the deprotonation process and thus to better understand the relative acidities described above, the electronic properties of the undeprotonated and the deprotonated conformers have been analyzed employing the natural population analysis (NPA), natural bond orbital (NBO), spin density, molecular orbitals (MOs) or/and electrostatic potential.

For Cu^+−adenine complexes, natural population analysis (NPA) shows a little charge transfer from adenine (0.17, 0.16 and 0.13 for **1a**, **3a** and **7a**, respectively, Table 5) to Cu^+, which can be attributed to the interaction from the ligand (N atom) lone pairs toward the 4s empty orbital of Cu^+. That is to say, in the Cu^+−adenine complex, copper is nearly one positively charged and adenine is an essentially neutral molecule. Thus, the deprotonation process of Cu^+−adenine is nearly the same as that of adenine; i.e., a proton is removed directly from the given sites on adenine fragment. However, in the case of Cu^{2+}−adenine, different situations are observed. For monodentate complexes **1b** and **3b**, NPA indicates a significant charge transfer (1.09 and 1.07, respectively, Table 5) from adenine to Cu^{2+}. Thus, copper behaves more as Cu^+ than as Cu^{2+}, whereas adenine behaves more as $A^{\bullet+}$ than as a neutral adenine. Moreover, the spin densities of **1b** and **3b** show that single electron essentially lies on adenine, not on the metal ion as is expected for a d^9 Cu^{2+} cation (see Figure 4). In agreement with NPA and spin density distribution, the open shell orbital in monodentate complex is localized at the adenine monomer, not at the Cu^{2+} cation as is well-known (see Figure 5 for MOs). Thus, the monodentate complexes could be regarded as Cu^+−$A^{\bullet+}$ rather than as Cu^{2+}-A. Similar findings have also been observed in the literature for guanine−, uracil−, thiouracil− and glycine−Cu^{2+} complexes.[4a,24,41] For bidentate complex **7b**, the spin density (Figure 4) and the open shell orbital (Figure 5) are more delocalized between the metal cation and adenine. NPA shows the charge transfer from adenine to Cu^{2+} is predicted to be 0.90, and thus, $q(Cu^{2+})$ is predicted to be 1.10 (Table 5), not 2 as is known. Therefore, the bidentate complex **7b** could also be regarded as Cu^+−$A^{\bullet+}$. That is, the interaction of Cu^{2+} with adenine leads to an oxidation of A to $A^{\bullet+}$, and Cu^{2+}−A really behaves as Cu^+−$A^{\bullet+}$ irrespective of N1-, N3- or N7-coordination. This is well reflected in the longer distance of Cu^{2+}−ligand bond and higher acidity of Cu^{2+}−adenine induced by the electrostatic repulsion between two positively charged fragments. Consequently, the final deprotonated Cu^{2+}−adenine ($[Cu-A(-H^+)]^+$) can be viewed as the interaction of Cu^+ (d^{10}) with the deprotonated $A^{\bullet+}$ ($[A(-H^+)]^{\bullet}$). Moreover, the similarity in spin density of the $[Cu-A(-H^+)]^+$ to that of the corresponding $[A(-H^+)]^{\bullet}$ confirms this assumption (Figure S).

As described above, N9−H group is the most acidic site for A and $A^{\bullet+}$. Thus, according to the assumption on the deprotonation process, N9−H should be the most acidic group in $Cu^{+/2+}$−adenine complexes for each coordination site. But only for N3-coordination, this is the case (for N1- and N7-coordination, the most acidic sites are N6−H^a and N6−H^b groups, respectively, and the acidity of C2−H is significantly enhanced). To highlight this relative acidity of $Cu^{+/2+}$−adenine complexes, the electrostatic potential and the natural bond orbital (NBO) for the relevant species have been performed on the base of the above deprotonation process. The electrostatic potential surfaces for $[A(-H^+)]^-$ and $[A(-H^+)]^{\bullet}$

are shown in Figure 6. The color at each point on these surfaces reflects the interaction energy between the deprotonated molecule and the metal cation at that point. The areas of red color indicate a negative region and are attractive to metal cation, and blue areas represent a positive region and are repulsive to metal cation. A cursory examination of the electrostatic potential surfaces for $[A(-H^+)]^-$ and $[A(-H^+)]^\bullet$ reveals that the ligand atom close to the deprotonation site is more red, whereas the ligand atom(s) remote to the deprotonation site is(are) less red, indicating that copper ion interaction with the ligand atom(s) close to the deprotonation site could stabilize the deprotonated structures to the full extent. Concretely, the regions around N1 and N6 of $[A(N6a)]^-$ and $[A(N6a)]^\bullet$ are encircled by more negative charge and thus are favorable for metal bidentate coordination, which could electrostatically stabilize the adjacent N6 anion. For the N7 site of $[A(N6b)]^-$ and $[A(N6b)]^\bullet$, this is also the case. A large negative cloud surrounds the regions around N6 and N7, making it favorable for metal ion bidentate bonding, and thereby stabilizing the deprotonated structures. This is consistent with the relative stabilities of the deprotonated structures and thus with the acidities of the coordination complex. Also, this can explain the depiction on the geometrical changes of the stable deprotonated conformers.

On the other hand, NBO analyses for the deprotonated structures show that in **1a/bN6a** or **7a/bN6b**, besides the electrostatic interaction between the metal cation and the $[A(-H^+)]^-/[A(-H^+)]^\bullet$ mentioned above, there are two dative bonds from the N1 and N6 lone pairs or the N6 and N7 lone pairs toward the 4s empty orbital of copper ion, which also contributes to stabilize the deprotonated structures. In **7a/bN6b** complex, the stronger interaction of $Cu^{+/2+}$ with $[A(-H^+)]^\bullet$ N7 and N6 is reflected in a significantly enhanced stability of the **7bN6b** complex, which is ~34.74 kcal/mol more stable than **7bN9**, although $[A(N6b)]^-/[A(N6b)]^\bullet$ is 18.4/5.0 kcal/mol less stable than $[A(N9)]^-/[A(N9)]^\bullet$. The situation for N6a-deprotonated **1a/b** is rather similar to that of **7a/bN6b**. Bidentate coordination of $Cu^{+/2+}$ with N1 and N6 provides the **1a/bN6a** about 17.0/23.0 kcal/mol more stability energy than **1a/bN9**, although $[A(N6a)]^-/[A(N6a)]^\bullet$ is ~18.0/5.0 kcal/mol less stable than $[A(N9)]^-$. All of these provide the evidence that in **1a**, **1b** or **7a** and **7b**, the most acidic group is N6−Ha or N6−Hb, not N9−H. Also, two dative bonds from the N1 and N6 loner pairs or the N6 and N7 loner pairs toward the 4s empty orbital of copper ion are the origin of the stabilities of **1a/bN6b** and **7a/bN6b** with respect to **3a/bN9**. For example, the stronger interaction of Cu^{2+} with $[A(-H^+)]^\bullet$ enhanced the stability of the **7bN6b** by ~10.2 kcal/mol compared with that for **3bN9**, although $[A(N6b)]^\bullet$ and **7b** are 3.0 and 18.4 kcal/mol less stable than $[A(N9)]^\bullet$ and **3b**, respectively. The situation for N6a-deprotonated $Cu^{+/2+}$−adenine is rather similar.

In addition, as shown in Figure 6, the C2 site of $[A(C2)]^-$ is surrounded by quite a large negative cloud around N1 and N3, which reveals that the C2 carbanion of adenine experiences a significant electrostatic repulsion from the N1 and N3 lone pairs. Such electrostatic repulsion makes the C2 carbanion unstable, suggesting that the acidity of C2−H in adenine is weak. However, the copper ion interaction with N1, C2 or N3 decreases the negative cloud around N1, C2 or N3 atom, making the ligand atom more positive, which could in turn electrostatically stabilize the C2 anion. The enhanced stabilization of the C2 carbanion means the coordination of copper to N1, C2 or N3 increases the acidity of C2−H group. Similarly, copper ion coordination to N7 also makes ligand atom more positive and thus could stabilize the C2 carbanion through conjugation effect. On the other hand, electrostatic potential clearly indicates that the N7 site of $[A(C2)]^-$ is less red than that of $[A(C2)]^\bullet$, which suggests that N7 coordination to copper(II) is more favorable than copper(I). That is to say, the C2−H group in **7b** is more acidic than that in **7a**. Also, NBO analyses indicate that in **1a/bC2** and **3ac2**, there is a strong σ bond between C2 and Cu^+. In the σ_{C2-Cu+} bond, the electron occupations are ~1.956. In the other C2 deprotonated structure, NBO analyses show a dative bond N3/N7 lone pair to the 4s empty orbital of copper ion. All of these σ bonds or dative bonds provide the strong stabilization to the deprotonated structures and thus are the origin of the strong acidity of C2−H group in coordination complexes. All above results are in good agreement with the higher acidity of C2−H group with respect to the neutral adenine.

On the other hand, as described above, $Cu^{+/2+}$ coordination to adenine N1 and Cu^+ coordination to adenine N3 take place in the same adenine's plane. However, $Cu^{+/2+}$ coordination to N1 in C2 deprotonated structures and Cu^+ coordination to N3 in N6 deprotonated structures do not take place in the same adenine's plane. NBO analysis reveals that in **1a/b** and **3a**, there is a dative bond from N1 or N3 lone pair to Cu 4s empty orbital. However, in **1a/bC2** and **3aC2** structures, C2 forms a σ bond with $Cu^{+/2+}$ and C2 rehybridizes from sp^2 to $sp^{2.98}$ (near sp^3). In **3aN6a** and **3aN6b**, N3 forms a σ bond with Cu 4s empty orbital, in which the bonding orbitals of N3 are $sp^{56.89}$ and $sp^{57.86}$, respectively. The electron occupations of N3−Cu^+ σ bonds in **3aN6a** and **3aN6b** are 1.697 and 1.694 e, respectively. Such bonding interactions and hybridizations suggest that these five structures are nonplanar, which are in good accordance with the geometrical description above.

Conclusions

In the present research, gas-phase deprotonation of $Cu^{+/2+}$−adenine complexes as well as adenine and adenine radical cation has been investigated theoretically. The result reveals that the acidities of C−H and N−H groups in $Cu^{+/2+}$−adenine are significantly enhanced relative to the neutral adenine. The acidic order for a given site on adenine and adenine derivatives is as follows: Cu^{2+}−adenine > $A^{\bullet+}$ > Cu^+−adenine > A. For A and $A^{\bullet+}$, the most acidic site is the N9−H group. However, for Cu^+−adenine and Cu^{2+}−adenine, only N3-coordination still remains N9−H acid. N1- and N7-coordination exhibits N6−H^a and N6−H^b acid, respectively. Moreover, for a given coordination site, Cu^{2+} greatly decreases the gap between the most acidic group and the least one with respect to that in the neutral adenine. Such dependencies of the acidities on the metal coordination region and oxidation state of copper suggest that the acidities of the active groups could be controlled by modulating the metal coordination site and the metal cation. Additionally, it is found that C2−H group is surprisingly acidic in the coordination complexes. Calculations in aqueous solution show that our results can be extrapolated to aqueous solution.

Analyses of the electronic property indicate that Cu^{2+}−adenine can be regarded as $Cu^+-A^{\bullet+}$ than as Cu^{2+}−A, which contributes to the highest acidity of Cu^{2+}−adenine among the adenine derivatives studied. However, in Cu^+−adenine, there is little charge transfer, and Cu^+ is essentially one positively charged and adenine is essentially a neutral molecule. On the other hand, electrostatic potential calculations of $[A(-H^+)]^-$ and $[A(-H^+)]^\bullet$ show that the removal of H^a or H^b from the

amino group provides a dative bond from the deprotonated N and the original coordination ligand to copper ion besides the electrostatic interaction between them and thereby stabilizes the $[A(-H^+)]^-/[A(-H^+)]^{\bullet}$. Furthermore, NBO analysis confirms the electrostatic potential result.

Acknowledgment. This work is supported by Scientific Research Reward Fund for Excellent Young and Middle-Aged Scientists in Shandong Province (No. 2006BS04006) and shandong-NSF (Z2003B01).

Supporting Information Available: Detailed spin densities of $[A(-H^+)]^{\bullet}$ and $Cu^{2+}-$adenine$(-H^+)$. This material is available free of charge via the Internet at http://pubs.acs.org.

References and Notes

(1) *Metal ions in biological systems: Interactions of metal ions with nucleotides, nucleix acids, and their constituents*; Sigel, A., Sigel, H. Eds.; Marcel Dekker: New York, 1996; Vol. 32.

(2) (a) Lippert, B. *Coord. Chem. Rev.* **2000**, *200−202*, 487. (b) Potaman, V. N.; Soyfer, V. N. *J. Biomol. Struct. Dyn.* **1994**, *11*, 1035. (c) Guschlbauer, W.; Chantot, J. F.; Thiele, D. *J. Biomol. Struct. Dyn.* **1990**, *8*, 491.

(3) (a) Saenger, W. *Principles of Nucleic Acids Structure*; Springer-Verlag: New York, 1984. (b) Egli, M.; Gessner, R. V. *Proc. Natl. Acad. Sci. U.S.A.* **1995**, *92*, 180. (c) Anwander, E. H. S.; Probst, M. M.; Rode, B. M. *Biopolymers* **1990**, *29A*, 757.

(4) (a) Noguera, M.; Bertran, J.; Sodupe, M. *J. Phys. Chem. A* **2004**, *108*, 333. (b) Burda, J. V.; Sponer, J.; Hobza, P. *J. Phys. Chem.* **1996**, *100*, 7250.

(5) (a) Zamora, F.; Kunsman, M.; Sabat, M.; Lippert, B. *Inorg. Chem.* **1997**, *36*, 1583. (b) Moussatova, A.; Vázquez, M.-V.; Martínez, A. *J. Phys. Chem. A* **2003**, *107*, 9415.

(6) Arpalahti, J.; Klika, K. D. *Eur. J. Inorg. Chem.* **1999**, 1199.

(7) Day, E. F.; Crawford, C. A.; Folting, K.; Dunbar, K. R.; Christon, G. *J. Am. Chem. Soc.* **1994**, *116*, 9449.

(8) (a) Šponer, J.; Sponer, J. E.; Gorb, L.; Leszczynski, J.; Lippert, B. *J. Phys. Chem. A* **1999**, *103*, 11406. (b) Griesser, R.; Kampf, G.; Kapinos, L. E.; Komeda, S.; Lippert, B.; Reedijk, J.; Sigel, H. *Inorg. Chem.* **2003**, *42*, 32.

(9) Lamsabhi, A. M.; Alcamí, M.; Mó, O.; Yáñez, M. *J. Phys. Chem. A* **2006**, *110*, 1943.

(10) Burda, J. V.; Šponer, J.; Hrabáková, J.; Zeizinger, M.; Leszczynski, J. *J. Phys. Chem. B* **2003**, *107*, 5349.

(11) Schröder, G.; Lippert, B.; Sabat, M.; Lock, C. J. L.; Faggiani, R.; Song, B.; Sigel, H. *J. Chem. Soc., Dalton Trans.* **1995**, 3767.

(12) Meiser, C.; Freisinger, E.; Lippert, B. *J. Chem. Soc., Dalton Trans.* **1998**, 2059.

(13) Faggiani, R.; Lippert, B.; Lock, C. J. L.; Speranzini, R. A. *Inorg. Chem.* **1982**, *21*, 3216.

(14) Faggiani, R.; Lock, C. J. L.; Lippert, B. *J. Am. Chem. Soc.* **1980**, *102*, 5418.

(15) Raymond, K. N. In *Bioinorganic Chemistry*, Bertini, I., Gray, H. B., Lippard, S. J., Selverstone Valentine, J. Eds.; University Science Books: Sausalito, CA, 1994; Chapter 1.

(16) Russo, N.; Toscano, M.; Grand, A. *J. Mass Spectrom.* **2003**, *38*, 265.

(17) (a) Drouin, R.; Rodríguez, H.; Gao, S. W.; Gebreyes, Z.; O'Connor, T. R.; Holmquist, G. P.; Akman, S. A. *Free Radiat. Biol. Med.* **1996**, *21*, 261. (b) Burrows, C. J.; Muller, J. G. *Chem. Rev.* **1998**, *98*, 1109.

(18) (a) Gao, Y. G.; Sriram, M.; Wang, A. H. J. *Nucl. Acid Res.* **1993**, *21*, 4093. (b) Srivatsan, S. G.; Parvez, M.; Verma, S. *J. Inorg. Biochem.* **2003**, *97*, 340–344.

(19) (a) Liang, Q.; Dedon, P. C. *Chem. Res. Toxicol.* **2001**, *14*, 416. (b) Bal, W.; Kasprzak, K. S. *Toxicol. Lett.* **2002**, *127*, 55. (c) Lee, D. H.; O'Connor, T. R.; Pfeifer, G. P. *Nucleic Acids Res.* **2002**, *30*, 3566.

(20) (a) Theophanides, T.; Anastassopoulou, J. *Crit. Rev. Oncol. Hematol.* **2002**, *42*, 57. (b) Bugella-Altamirano, E.; Choquesillo-Lazarte, D.; González-Pérez, J. M.; Sánchez-Moreno, M. J.; Marín-Sánchez, R.; Martín-Ramos, J. D.; Covelo, B.; Carballo, R.; Castiñeiras, A.; Niclüs-Gutiérrez, J. *Inorg. Chim. Acta* **2002**, *339*, 160.

(21) Geierstanger, B. H.; Kagawa, T. F.; Chen, S. L.; Quigley, G. J.; Ho, P. S. *J. Biol. Chem.* **1991**, *266*, 20185.

(22) Chandra, A. K.; Nguyen, M. T.; Uchimaru, T.; Zeegers-Huyskens, T. *J. Phys. Chem. A* **1999**, *103*, 8853.

(23) Nguyen, M. T.; Chandra, A. K.; Zeegers-Huyskens, T. *J. Chem. Soc., Faraday Trans.* **1998**, *94*, 1277.

(24) Lamsabhi, A. M.; Alcamí, M. T.; Mo, O.; Yánez, M.; Tortajada, J. *ChemPhysChem* **2004**, *5*, 1871.

(25) (a) Marino, T.; Toscano, M.; Russo, N.; Grand, A. *Int. J. Quantum Chem.* **2004**, *98*, 347. (b) Noguera, M.; Branchadell, V.; Constantino, E.; Rı′os-Font, R.; Sodupe, M.; Rodrâguez-Santiago, L. *J. Phys. Chem. A* **2007**, *111*, 9823.

(26) Song, B.; Zhao, J.; Griesser, R.; Meiser, C.; Sigel, H.; Lippert, B. *Chem. Eur. J.* **1999**, *5*, 2374.

(27) Fernández-Botello, A.; Griesser, R.; Holý, A.; Moreno, V.; Sigel, H. *Inorg. Chem.* **2005**, *44*, 5104.

(28) Xing, D.; Chen, X.; Bu, Y. *New J. Chem.* **2007**, *31*, 1514.

(29) (a) Sharma, S.; Lee, J. K. *J. Org. Chem.* **2002**, *67*, 8360. (b) Sharma, S.; Lee, J. K. *J. J. Org. Chem.* **2004**, *69*, 7018.

(30) Montgomery, J. A., Jr.; Frisch, M. J.; Ochterski, J.; Petersson, G. A. *J. Chem. Phys.* **1999**, *110*, 2822.

(31) Curtiss, L. A.; Redfern, P. C.; Raghavachari, K.; Pople, J. A. *J. Chem. Phys.* **2001**, *114*, 108.

(32) Meng, Z.; Dölle, A.; Carper, W. R. *J. Mol. Struct.: THEOCHEM* **2002**, *585*, 119.

(33) Rappe, A. K.; Bernstein, E. R. *J. Phys. Chem. A* **2000**, *104*, 6117.

(34) Foster, J. P.; Weinhold, F. *J. Am. Chem. Soc.* **1980**, *102*, 7211.

(35) Reed, A. E.; Weinhold, F. *J. Chem. Phys.* **1983**, *78*, 4066.

(36) (a) Reed, A. E.; Weinstock, R. B.; Weinhold, F. *J. Chem. Phys.* **1985**, *83*, 735. (b) Reed, A. E.; Weinhold, F. *J. Chem. Phys.* **1985**, *83*, 1736.

(37) Reed, E.; Curtiss, L. A.; Weinhold, F. *Chem. Rev.* **1988**, *88*, 899.

(38) (a) Miertus, S.; Scrocco, E.; Tomasi, J. *Chem. Phys.* **1981**, *55*, 117. (b) Miertus, S.; Tomasi, J. *Chem. Phys.* **1982**, *65*, 239. (c) Cossi, M.; Barone, V.; Cammi, R.; Tomasi, J. *Chem. Phys. Lett.* **1996**, *255*, 327. (d) Mennucci, B.; Tomasi, J. *J. Chem. Phys.* **1997**, *106*, 5151.

(39) (a) Becke, A. D. *J. Chem. Phys.* **1993**, *98*, 5648. (b) Lee, C.; Yang, W.; Parr, R. G. *Phys. Rev. B* **1988**, *37*, 785. (c) Stephens, P. J.; Devlin, F. J.; Chabalowski, C. F.; Frisch, M. J. *J. Phys. Chem.* **1994**, *98*, 11623.

(40) Frisch, M. J.; Trucks, G. W.; Schlegel, H. B.; Scuseria, G. E.; Robb, M. A.; Cheeseman, J. R.; Montgomery, J. A., Jr.; Vreven, T.; Kudin, K. N.; Burant, J. C.; Millam, J. M.; Iyengar, S. S.; Tomasi, J.; Barone, V.; Mennucci, B.; Cossi, M.; Scalmani, G.; Rega, N.; Petersson, G. A.; Nakatsuji, H.; Hada, M.; Ehara, M.; Toyota, K.; Fukuda, R.; Hasegawa, J.; Ishida, M.; Nakajima, T.; Honda, Y.; Kitao, O.; Nakai, H.; Klene, M.; Li, X.; Knox, J. E.; Hratchian, H. P.; Cross, J. B.; Bakken, V.; Adamo, C.; Jaramillo, J.; Gomperts, R.; Stratmann, R. E.; Yazyev, O.; Austin, A. J.; Cammi, R.; Pomelli, C.; Ochterski, J. W.; Ayala, P. Y.; Morokuma, K.; Voth, G. A.; Salvador, P.; Dannenberg, J. J.; Zakrzewski, V. G.; Dapprich, S.; Daniels, A. D.; Strain, M. C.; Farkas, O.; Malick, D. K.; Rabuck, A. D.; Raghavachari, K.; Foresman, J. B.; Ortiz, J. V.; Cui, Q.; Baboul, A. G.; Clifford, S.; Cioslowski, J.; Stefanov, B. B.; Liu, G.; Liashenko, A.; Piskorz, P.; Komaroni, I.; Martin, R. L.; Fox, D. J.; Keith, T.; Al-Laham, M. A.; Peng, C. Y.; Nanayakkara, A.; Challacombe, M.; Gill, P. M. W.; Johnson, B.; Chen, W.; Wong, M. W.; Gonzalez, C.; Pople, J. A. *Gaussian 03*, revision D.01; Gaussian Inc.: Wallingford, CT, 2004.

(41) Georgieva, I.; Trendafilova, N.; Rodríguez-Santiago, L.; Sodupe, M. *J. Phys. Chem. A* **2005**, *109*, 5668.

JP800256V